Available online at www.sciencedirect.com

ScienceDirect

Biochimica et Biophysica Acta 1758 (2006) 1085 – 1093

BIOCHIMICA ET BIOPHYSICA ACTA

BBA

www.elsevier.com/locate/bbamem

Review

Three distinct roles of aquaporin-4 in brain function revealed by knockout mice

A.S. Verkman *, Devin K. Binder, Orin Bloch, Kurtis Auguste, Marios C. Papadopoulos [1]

Departments of Medicine and Physiology, Cardiovascular Research Institute, 1246 Health Sciences East Tower, Box 0521, University of California, San Francisco, CA 94143-0521, USA

Received 10 January 2006; received in revised form 26 January 2006; accepted 2 February 2006
Available online 10 March 2006

Abstract

Aquaporin-4 (AQP4) is expressed in astrocytes throughout the central nervous system, particularly at the blood–brain and brain–cerebrospinal fluid barriers. Phenotype analysis of transgenic mice lacking AQP4 has provided compelling evidence for involvement of AQP4 in cerebral water balance, astrocyte migration, and neural signal transduction. AQP4-null mice have reduced brain swelling and improved neurological outcome in models of (cellular) cytotoxic cerebral edema including water intoxication, focal cerebral ischemia, and bacterial meningitis. However, brain swelling and clinical outcome are worse in AQP4-null mice in models of vasogenic (fluid leak) edema including cortical freeze-injury, brain tumor, brain abscess and hydrocephalus, probably due to impaired AQP4-dependent brain water clearance. AQP4 deficiency or knock-down slows astrocyte migration in response to a chemotactic stimulus in vitro, and AQP4 deletion impairs glial scar progression following injury in vivo. AQP4-null mice also manifest reduced sound- and light-evoked potentials, and increased threshold and prolonged duration of induced seizures. Impaired K^+ reuptake by astrocytes in AQP4 deficiency may account for the neural signal transduction phenotype. Based on these findings, we propose modulation of AQP4 expression or function as a novel therapeutic strategy for a variety of cerebral disorders including stroke, tumor, infection, hydrocephalus, epilepsy, and traumatic brain injury.

Keywords: AQP4; Water transport; Transgenic mouse; Brain edema; Cell migration; Epilepsy

Contents

1. Introduction

Excess accumulation of brain water, cerebral edema, is of central importance in the pathophysiology of a wide range of central nervous system (CNS) abnormalities such as stroke, tumor, infection, hydrocephalus, and traumatic brain injury [1]. Cerebral edema produces elevated intracranial pressure (ICP),

* Corresponding author. Tel.: +1 415 476 8530; fax: +1 415 665 3847.
E-mail address: verkman@itsa.ucsf.edu (A.S. Verkman).
URL: http://www.ucsf.edu/verklab (A.S. Verkman).
[1] Present address: St. George's University, London, UK.

0005-2736/$ - see front matter © 2006 Elsevier B.V. All rights reserved.
doi:10.1016/j.bbamem.2006.02.018

potentially leading to brain ischemia, herniation and death. Despite a large body of empirical data on brain edema and its causes and consequences, current treatments for brain edema such as hyperosmolar agents and surgical decompression have changed little since their introduction more than 80 years ago [2].

Aquaporin-4 (AQP4) is a water-selective transporter originally cloned by our lab in 1994 from lung tissue [3] and shown to be expressed strongly in brain [4]. AQP4 is expressed in astrocytes and ependymal cells throughout the brain and spinal cord, particularly at sites of fluid transport at the pial and ependymal surfaces in contact with the cerebrospinal fluid (CSF) in the subarachnoid space and the ventricular system (Fig. 1) [5,6]. Polarized AQP4 expression is found in astrocytic foot processes in direct contact with blood vessels. In spinal cord, AQP4 expression is high in gray matter where numerous AQP4 dense processes are found in direct contact with neuronal cell bodies and synapses [7,8]. This expression pattern suggests AQP4 involvement in the movement of water between blood and brain, and between brain and CSF compartments. Interestingly, AQP4 is a structural component of membrane orthogonal arrays of particles (OAPs), which are regularly spaced intramembrane particles seen in freeze-fracture electron micrographs (FFEM). Based on AQP4 expression in the same cells in which OAPs were identified, we originally proposed that AQP4 is the OAP protein [9]. Support for this hypothesis came from FFEM on stably transfected CHO cells [10], and from the absence of orthogonal arrays in brain, kidney and skeletal muscle from AQP4-null mice [11].

This review is focused on the role of AQP4 in brain function, as deduced largely from phenotype analysis of transgenic mice deficient in AQP4. These mice, originally generated by targeted gene disruption in 1997 and shown to have only a very mild urinary concentrating defect [12], have normal brain structure, vascular anatomy, baseline ICP, intracranial compliance, and blood–brain barrier function [13,14]. We review evidence for involvement of AQP4 in cytotoxic brain edema, as well as in several unanticipated functions, including vasogenic brain edema, glial cell migration, and neural signal transduction.

2. Involvement of AQP4 in brain edema

The two main types of cerebral edema are cellular (cytotoxic) and vasogenic [15]. Cellular edema occurs when fluid flows from the vascular compartment, through intact blood–brain barrier and astrocytic foot processes, and accumulates primarily in astrocytes [16]. In vasogenic edema, the blood–brain barrier becomes leaky, permitting the entry of plasma fluid into the brain ECS. Edema fluid is eliminated from the brain through the glia limitans externa into the subarachnoid space, through the glia limitans interna and ependyma into the ventricles, and through the blood–brain barrier into the blood [15,17,18]. Hydrocephalic edema, which is sometimes classified as a specialized type of vasogenic brain edema [1], arises from impaired escape of CSF into the blood by obstruction of CSF drainage.

We initially tested the hypothesis that AQP4 plays a role in the early accumulation of brain water in response to established neurological insults producing cytotoxic brain edema, including acute water intoxication [13]. Brains from AQP4 null mice show reduced osmotic water permeability as measured in isolated membrane vesicles [12], brain slices [19], and intact brain [20]. Also, water permeability was seven-fold reduced in primary astrocyte cultures from AQP4-deficient mice as measured by a

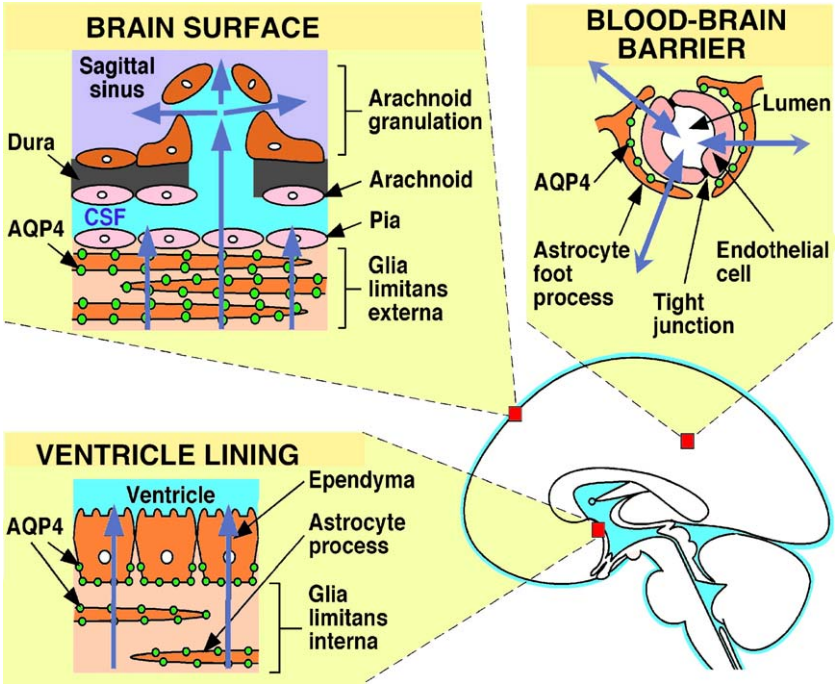

Fig. 1. Schematic showing site of AQP4 expression in brain and three pathways for water movement out of brain in vasogenic edema.

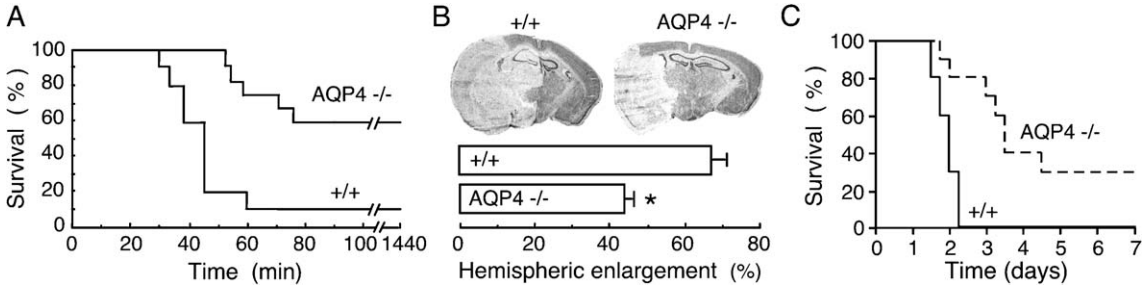

Fig. 2. Reduced brain edema and improved outcome in AQP4 null mice in models of cytotoxic brain edema. (A) Survival of wildtype vs. AQP4 knockout mice after acute water intoxication produced by intraperitoneal water injection. (B) (top) Brain sections of mice at 24 h after ischemic stroke produced by permanent middle cerebral artery occlusion. Note midline shift and marked edema in brain from wildtype mice. (bottom) Average hemispheric enlargement expressed as a percentage determined by image analysis of brain sections. (C) Mouse survival in a bacterial model of meningitis produced by cisternal injection of Streptococcus. From references [13,22].

calcein fluorescence quenching method [21], indicating that AQP4 provides the predominant pathway for water movement in astrocytes. AQP4 deletion in mice conferred remarkable protection from cytotoxic brain edema. The survival of AQP4 null mice after water intoxication produced by intraperitoneal water infusion (reducing serum Na^+ to 100–105 mM) was greatly improved (Fig. 2A), with significantly reduced swelling in astrocytic foot processes from AQP4 null mice. In addition, at 24 h after brain ischemia produced by permanent middle cerebral artery occlusion (suture occlusion model) there was improved clinical outcome and significantly reduced brain swelling (Fig. 2B). We recently studied the role of AQP4 in a bacterial meningitis model of cytotoxic brain edema produced by cisternal injection of streptococcus [22]. Mice lacking AQP4 showed remarkably improved survival (Fig. 2C) and reduced brain water accumulation and ICP elevation, despite comparable bacterial load and immune response. Together, these results provide direct functional evidence for involvement of AQP4 in cytotoxic brain edema, and suggest the potential use of AQP4-selective inhibitors to reduce brain water accumulation in cytotoxic edema.

In a subsequent study in dystrophin null (*mdx*) mice, which have reduced AQP4 expression in astrocyte foot processes [23], there was similar protection against water intoxication, though significant differences such as death in all wildtype and *mdx* mice. The differences in survival between the dystrophin null mice and the AQP4-null mice may be related to baseline morphological alterations found in the dystrophin null mice such as increased blood–brain barrier permeability [24], which may enhance the transport of water from the intravascular space to the brain and hence worsen cerebral edema and clinical outcome.

Because AQP4 permits bidirectional water transport, we hypothesized that AQP4 may facilitate the removal of excess brain water in vasogenic (non-cellular) brain edema. In support of this hypothesis, we found markedly elevated intracranial pressure (ICP) and brain water content in AQP4-deficient mice after continuous slow intraparenchymal fluid infusion of isosmolar artificial cerebrospinal fluid [14].

AQP4-dependent clearance of excess brain water in vasogenic brain edema was supported by data from three additional models. In a freeze-injury model of vasogenic brain edema, AQP4-deficient mice had worse clinical outcome, higher ICP, and greater brain water accumulation, though comparable blood–brain barrier leakiness (as assessed by Evans blue dye extravasation) [14]. To investigate the clinical relevance of these observations, we developed a model of brain tumor edema involving stereotaxic implantation of melanoma cells. Melanoma cells were injected into the right striatum as diagrammed (Fig. 3A, top). The injected cells produced a rapidly growing, well-demarcated dark tumor in wildtype and AQP4 null mice

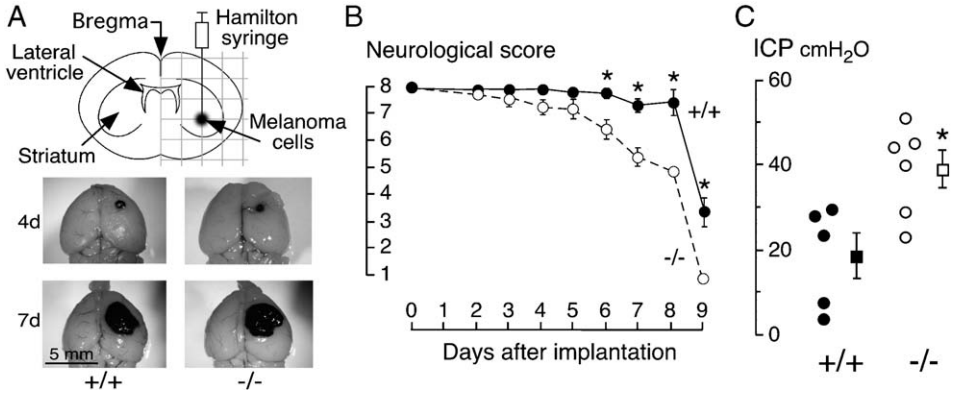

Fig. 3. Increased ICP and worse clinical outcome in AQP4 null mice with melanoma brain tumor. (A) (top) Site of injection of melanoma cells. (bottom) Tumor size at 4 and 7 days after implantation showing similar-sized tumors in wildtype and AQP4 null mice. (B) Neurological score and (C) ICP measured at 7 days (mean ± S.E., $*P<0.001$ for neurological scores, $*P< 0.02$ for ICP). From reference [58].

(Fig. 3A, bottom). Tumor volume, as assessed at 7 days post-implantation by optical imaging of 1-mm thick sections of formalin-fixed brain parenchyma, did not differ significantly in wildtype vs. AQP4 null mice. However, the AQP4 null mice had significantly worse neurological score at days 6–8 (Fig. 3B), as well as higher ICP (Fig. 3C) [14]. Recently, in another clinically relevant model of vasogenic brain edema, staphylococcal brain abscess, we found significantly worse clinical outcome in the AQP4 null mice, with greater ICP elevation and brain water accumulation [25]. Together, these results support a novel role for AQP4 in the resolution of vasogenic brain edema by a transcellular route.

The involvement of AQP4 in clearance of excess brain water is an unanticipated finding because AQP4 is water-selective. Vasogenic edema is generally believed to be cleared primarily by bulk flow of fluid through the extracellular space and glia limitans into the ventricles and subarachnoid space, and to a lesser extent through astrocyte foot processes and capillary endothelium into the blood [15,17,18]. Another proposed but controversial route for clearance of edema fluid is movement from brain parenchyma into Virchow–Robin perivascular spaces, which are CSF-filled spaces that communicate with the subarachnoid space [26]. AQP4-rich astrocyte processes of the glia limitans interna and glia limitans externa form a dense mesh at the brain–CSF boundaries and ultrastructural studies show that these long astrocytic processes are separated by narrow (<20 nm) intercellular clefts and are interconnected by gap junctions [27]. Because of the long diffusion path, the glia limitans is likely a significant permeability barrier to the extracellular flow of water and solutes. The impaired clearance of excess brain water in AQP4 null mice in vasogenic edema suggests that AQP4 provides a low resistance transcellular route, which allows edema fluid to move across the astrocyte cell membranes of the glia limitans into the CSF. We propose that enhanced elimination of excess brain water through this transcellular pathway would also accelerate the removal of associated solutes by creating a solute concentration gradient between brain parenchyma and CSF. Another possibility might be altered size of processes in the glia limitans in AQP4 deficiency that reduces fluid clearance.

We recently investigated the role of AQP4 in progression of hydrocephalus. Hydrocephalus occurs as the result of an imbalance between CSF production and absorption, leading to accumulation of extraparenchymal fluid, expansion of the ventricular system, and ICP elevation. Non-communicating hydrocephalus is caused by obstruction within the ventricular system, such as a tumor, that prevents CSF proximal to the obstruction from draining into the subarachnoid space where it is absorbed. Communicating hydrocephalus results from impaired absorption of CSF despite patent CSF pathways. Both communicating and non-communicating (obstructive) hydrocephalus may be congenital or acquired secondary to trauma, tumor, hemorrhage, or infection. Current primary treatment for hydrocephalus involves surgical drainage and diversion of excess CSF.

Based on rat models, we developed a reproducible mouse model of progressive obstructive hydrocephalus [28]. Injection of kaolin into the cisterna magna resulted in CSF accumulation and ventricular enlargement. By 5 days post-injection there was significant expansion of the lateral, third, and fourth ventricles in wildtype mice (Fig. 4A). Lateral ventricle volume in wild-type mice was <0.1 mm^3 prior to kaolin administration, increasing to >5 mm^3 at 7 days post-injection. Ventricular enlargement was significantly greater in AQP4 null mice at 3 and 5 days post-injection, but not at 1 day (Fig. 4B). ICP was measured using a

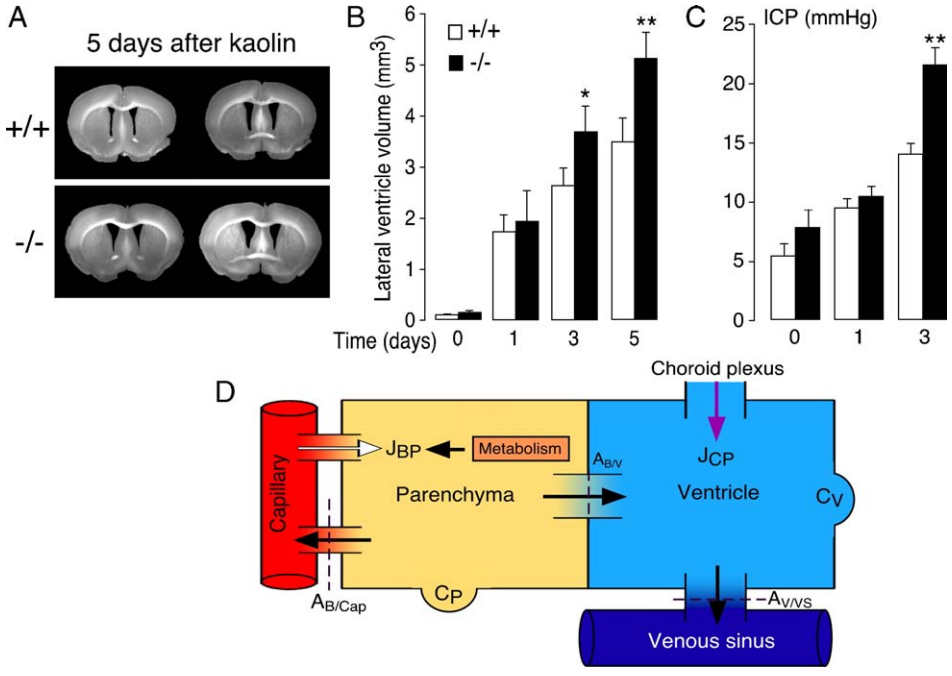

Fig. 4. Accelerated progression of hydrocephalus in AQP4 null mice. (A) Coronal sections of fixed brains from wildtype (top) and AQP4 null (bottom) mice at 5 days after kaolin injection. (B) Lateral ventricle volume over 5 days following cisternal kaolin injection. (C) ICP following kaolin injection. (D) Multi-compartment model of hydrocephalus. White arrows indicate fixed flows and black arrows indicate positive direction of pressure-dependent flows. From reference [28].

solid-state micropressure transducer introduced into the brain parenchyma through a small cranial burr hole. At 3 days following kaolin injection, ICP increased by ~12 mm Hg above baseline in wildtype mice (Fig. 4C). Greater ICP elevation was seen in AQP4 null mice, such that it was not possible to measure ICP in the null mice at 5 days because of CSF leakage caused by drilling the small burr hole required to introduce the measuring device. Neither ventricular size nor ICP differed significantly in wildtype vs. AQP4 null mice at 1 day post-injection, where the brain has relatively high compliance and fluid entry into the brain dominates over exit.

The experimental data show that AQP4 deletion in mice accelerates the progression of obstructive hydrocephalus. As diagrammed in Fig. 4D, a mathematical model of progressive hydrocephalus was developed to understand the experimental data and to model predicted effects of upregulation of AQP4 expression. The model, which is described in detail in ref. 28, includes CSF production and drainage, as well as water transfer among ventricular, parenchymal, capillary and venous compartments. Obstructive hydrocephalus was modeled by reduction of hydrostatically driven fluid transport from ventricle to venous sinus, and AQP4 deletion was modeled by reduction in permeability of the capillary–parenchymal and parenchymal–ventricular barriers. The model accurately reproduced the greater severity of hydrocephalus in AQP4 null vs. wild-type mice, and predicted a much reduced severity if AQP4 expression/function were increased.

3. Involvement of AQP4 in glial cell migration

We recently discovered a new function of AQP4 in facilitating astrocyte migration. The original motivation that led to this work was the observation of strong AQP1 expression in tumor microvessels. We found remarkably impaired tumor growth in AQP1 null mice after subcutaneous or intracranial tumor cell implantation, with reduced tumor vascularity and extensive necrosis [29]. Although adhesion and proliferation were similar in primary cultures of aortic endothelia from wildtype vs. AQP1 null mice, cell migration was greatly impaired in AQP1-deficient cells, with abnormal vessel formation in vitro. Stable transfection of non-endothelial cells with AQP1 or AQP4 accelerated cell migration and in vitro wound healing. Motile AQP1-expressing cells had prominent membrane ruffles at their leading edge with polarization of AQP1 protein to lamellipodia, where rapid water fluxes occur. The findings supported a fundamental role of water channels in cell migration, which we proposed occurs in many cell types expressing aquaporins. In the brain, astrocyte cell migration is important in glial scar formation [30–33]. Rapid formation of a glial scar can be beneficial, by restoring the blood–brain barrier, preventing neuronal death, and limiting influx of inflammatory cells into the brain [34,35]. Perhaps more often glial scar formation has deleterious effects, including inhibition of axonal sprouting in damaged brain and spinal cord [36], and prevention of access of drugs or genes to a lesion [37].

Two types of assays were done to study in vitro migration of cultured astrocytes from wild-type and AQP4-null mouse brain: 'transwell migration' and 'wound healing'. Using a modified Boyden chamber containing a porous membrane filter [38], astrocytes suspended in culture medium containing 1% serum were introduced into the upper chamber, with the lower chamber containing medium with 10% serum as chemoattractant. After 6 h, cells were stained and counted, and non-migrated cells scraped off the upper surface of the filter to count migrated cells on the bottom surface. As shown in Fig. 5A, this assay revealed slowed migration of AQP4 null vs. wildtype astroglia. In a

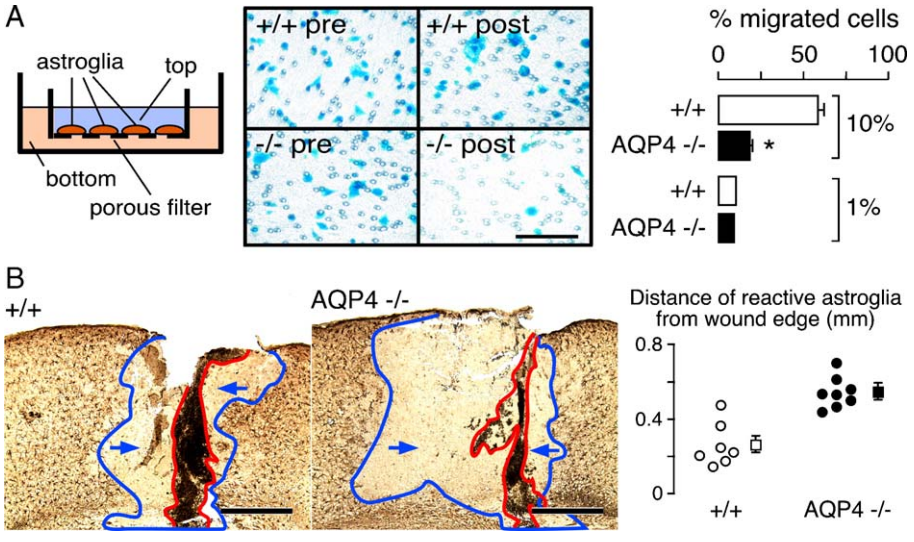

Fig. 5. Slowed migration of AQP4-deficient astroglia. (A) Left, schematic of Boyden chamber in which cells migrate downward through a porous filter in response to a chemotactic stimulus. Middle, representative photos of transwell migration assay showing Coomassie blue-stained wildtype (+/+) and AQP4 null (−/−) astroglia before (pre) and after (post) scraping the non-migrated cells. Scale bar = 100 μm. Right, data summary of migration experiments towards 10% serum (*P<0.001) or 1% serum. (B) Left, astroglial cell migration after stab injury in vivo. Astroglial front (blue line) and margin of stab injury (red line) in wildtype and AQP4 null (E) mouse at 3 days after stab. Arrows show direction of migration of the reactive astroglial front. GFAP immunostaining (brown). Right, average distance of reactive astroglial front from the edge of the stab wound at 3 days after stab injury (*P<0.001). Scale bars = 400 μm. From reference [38].

second assay of cell migration, confluent astroglial monolayers were wounded by scraping a strip of cells with a micropipette tip [38]. Wound healing was also greatly slowed in astrocytes from AQP4-deficient mice. Results similar to those in AQP4-null astrocytes were found in astrocytes from wildtype mice after RNAi knock-down of AQP4. Also, AQP4-null astrocytes had fewer lamellipodia than wildtype astrocytes, which showed AQP4 protein polarization to the leading edge of migrating cells.

The possible involvement of AQP4 in glial scar formation in vivo was investigated using a model of stereotactically guided stab injury to the cerebral cortex [30,32,35,38,39]. At various time points, reactive astrocytes were identified by their stellate morphology after immunostaining for GFAP. We found significantly impaired glial cell migration in AQP4 null mice, seen as an increased margin between strongly GFAP-positive cells and the lesion site (Fig. 5B). These results provided in vivo evidence for AQP4-dependent astrocyte migration. Tracking of individual wild-type vs. AQP4-deficient astrocytes in brain will be useful in exploring further the role of AQP4 in glial cell migration.

The importance of water fluxes across the plasma membrane in causing localized swelling of lamellipodia has been discussed extensively in the early literature on cell migration [40,41]. In support of this mechanism as applied to AQP4 migration in astrocytes, we found that the speed of astrocyte migration can be altered by a small osmotic gradient in the extracellular medium, resulting in accelerated astrocyte migration towards hypo-osmolality. We suggest that AQP4 accelerates astrocyte migration by increasing plasma membrane water permeability, which in turn increases the transmembrane water fluxes that take place during cell movement. This hypothesis could explain the observation that AQP4 deletion slows the rapid changes in cell shape that take place at the leading end of migrating astrocytes. It has been suggested that the generation of osmoles produced by rapid actin depolymerization drives the entry of water into the leading end of migrating cells [40], possibly in concert with transmembrane ionic movements [42,43]. The osmotic influx of water across the plasma membrane expands the leading end of the cell, which is followed by actin polymerization to stabilize the membrane protrusion [40]. It will be useful to measure transmembrane water movement directly in cell protrusions.

4. Involvement of AQP4 in neural signal transduction

The brain extracellular space (ECS) comprises ~20% of brain tissue volume, consisting of a jelly-like matrix in which neurons, glial cells, and blood vessels are embedded. The ECS contains ions, neurotransmitters, metabolites, peptides, and extracellular matrix molecules, forming the microenvironment for all cells in the brain. The ECS also serves as a critical communication channel, in which populations of neurons and glial cells interact by specialized synaptic contacts (neuron to neuron) as well as by extrasynaptic diffusion of ions and neurotransmitters. Communication between neurons and glia occurs via diffusible messengers, metabolites, and ions in the ECS [44–46]. For example, neuronal activity is associated with depolarization of neurons and adjacent glial cells, and with increased extracellular glutamate and K^+, which can synchronize neuronal activity as well as activate glial metabolism and signaling [47–50]. Recent studies have also demonstrated direct synaptic contacts onto glial cells [51,52].

We have obtained several lines of evidence for AQP4 involvement in neural signal transduction from phenotype analysis of AQP4-null mice. Based on the expression of AQP4 in supportive epithelial cells adjacent to (electrically-excitable) hair cells in rat inner ear, we investigated the involvement of AQP4 in auditory signal transduction [53]. Auditory brainstem response (ABR) thresholds were remarkably increased by >20 dB in AQP4 null mice compared to wildtype mice. Also, light evoked potentials (b-wave amplitude measured by electroretinography) were reduced in AQP4 null mice [54], consistent with the view that the AQP4-expressing Müller (glia-like) cells are functionally coupled to the transducing bipolar cells. In brain, seizure susceptibility in response to the convulsant (GABA antagonist) pentylenetetrazol (PTZ) was remarkably increased in AQP4-null mice [55]. At 40 mg/kg PTZ, all wildtype mice exhibited seizure

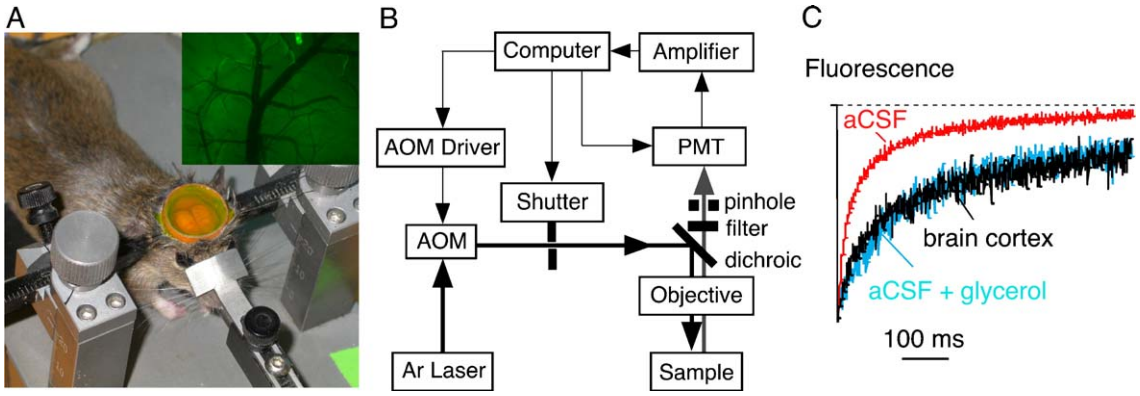

Fig. 6. In vivo cortical surface photobleaching. (A) Mouse brain surface exposed to FITC-dextran with dura intact following craniectomy and fluorescence imaging of cortical surface after loading with FITC-dextran (inset). (B) Photobleaching apparatus. A laser beam is modulated by an acousto-optic modulator and directed onto the surface of the cortex using a dichroic mirror and objective lens. Emitted fluorescence is focused through a pinhole and detected by a gated photomultiplier (PMT). (C) In vivo fluorescence recovery in cortex of wildtype mouse shown in comparison to aCSF and 30% glycerol in aCSF. From reference [57].

activity, whereas 6 out of 7 AQP4 null mice did not exhibit seizure activity; at 50 mg/kg PTZ, both groups exhibited seizure activity; however, the latency to generalized (tonic–clonic) seizures was greater in AQP4 null mice. In recent studies, in vivo EEG characterization of electrically-induced seizures following hippocampal stimulation indicated greater threshold and remarkably longer seizure duration in AQP4 null mice compared to wildtype mice [56]. These phenotype observations suggested involvement of AQP4 in neural signal transduction, which we proposed could be related to AQP4-dependent K^+ dynamics in the ECS. We therefore developed methodologies to test the hypothesis that ECS volume and/or K^+ uptake by glial cells is altered in AQP4 deficiency.

Evidence for an expanded ECS in AQP4 deficiency was obtained using a surface photobleaching method to measure the diffusion of fluorescently-labeled macromolecules [57]. ECS in mouse brain was labeled by exposure of the intact dura to fluorescein-dextrans (M_r 4, 70 and 500 kDa) after craniectomy (Fig. 6A). Fluorescein-dextran diffusion was detected by fluorescence recovery after laser-induced cortical photobleaching using confocal optics, as shown in Fig. 6B. FITC-dextran diffusion was slowed ~3-fold in brain ECS relative to solution (aCSF, artificial cerebrospinal fluid) (Fig. 6C). The cortical photobleaching approach was applied to problems of brain edema, seizure initiation, and AQP4 deficiency. Cytotoxic brain edema (produced by water intoxication) or seizure activity (produced by convulsants) slowed diffusion by >10-fold and created dead-space microdomains in which free diffusion was prevented. The hindrance to diffusion was greater for the larger fluorescein dextrans. Interestingly, slowed ECS diffusion preceded electroencephalographic seizure activity. Diffusion of FITC-dextrans was significantly accelerated in AQP4 null mice, suggesting an expanded ECS. In follow-up studies, cortical surface photobleaching was used to demonstrate accelerated macromolecule diffusion in the expanded ECS in vasogenic edema [58]. We recently extended this approach to quantify anisotropic diffusion in spinal cord and brain by 'elliptical photobleaching' in which bleaching was done with an elliptical laser spot (produced by cylindrical optics) [59]; the contribution of ECS geometry vs. matrix composition in slowing macromolecular diffusion was estimated for the first time.

We recently obtained direct in vivo evidence for impaired K^+ reuptake from the ECS in AQP4 deficiency. A long-wavelength K^+-sensing fluorescent indicator, TAC-Red (Fig. 7A), was synthesized, which consisted of a triazacryptand K^+ ionophore coupled to a 3,6-bis(dimethylamino) xanthylium chromophore [60]. As shown in Fig. 7B, TAC-Red fluorescence increased by ~15-fold with increasing K^+ in the range 0–40 mM, and had little sensitivity to Na^+ or to pH in the range 6–8. More than 90% of the fluorescence increase in response to an increase in $[K^+]$ occurred in under 1 ms. The ECS of mouse brain surface was stained with TAC-Red by exposing the intact dura (after craniectomy) for 5 min to aCSF containing TAC-Red. The TAC-red-stained brain cortex was brightly red fluorescent, with fairly uniform parenchymal staining. A pin prick model of cortical spreading depression produced propagating K^+ waves at the cortical surface. Some frames of a video are shown (in pseudocolor) in Fig. 7C, showing a wave of increasing K^+

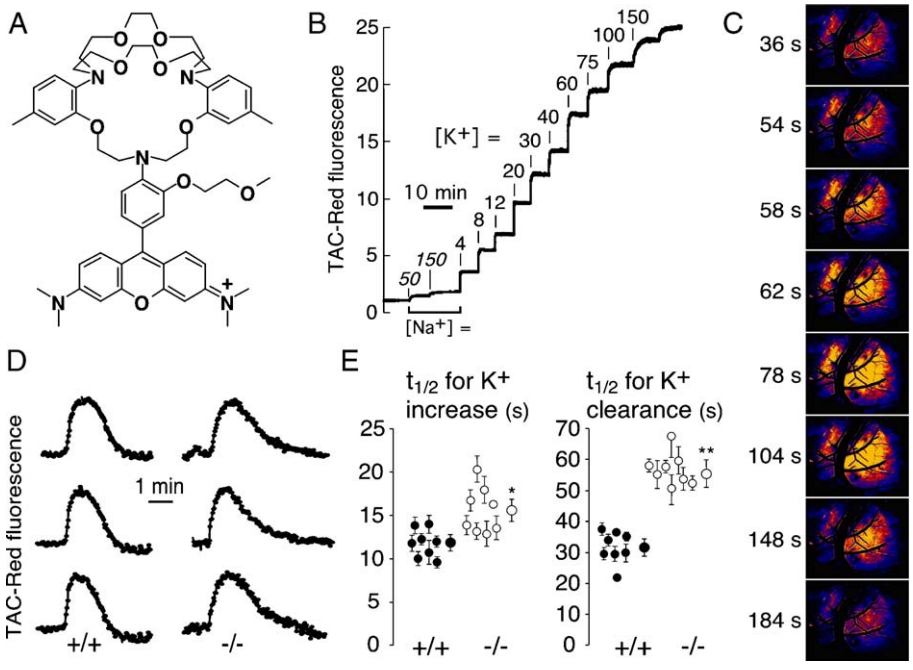

Fig. 7. Evidence for impaired glial cell K^+ uptake from the ECS in AQP4 deficiency. (A) Chemical structure of TAC-Red. (B) Titration of TAC-Red showing serial additions of NaCl (50 and 150 mM), following by additions of KCl. (C) Serial images of brain cortex at indicated times after initiation of cortical spreading depression by pin prick. TAC-Red fluorescence is shown in pseudocolor, with increasing intensities scaled as black–blue–red–yellow–white. (D) Time course of TAC-Red fluorescence at single points in wild-type and AQP4 null mice (each curve from different mouse) following initiation of spreading depression. (E) Half-times ($t_{1/2}$) for the increase (K^+ release) and return to baseline (K^+ reuptake) in TAC-Red fluorescence. Each point is the average (±S.E.M.) from twelve different locations per mouse (S.E., 8 mice, $*P<0.05$, $**P<0.001$). From reference [60].

following pin-prick stimulation. Using this method, we compared the kinetics and propagation velocity of K^+ waves in wildtype vs. AQP4 null mice. Fig. 7D shows broader K^+ wave profiles in the AQP4-deficient mice. Fig. 7E summarizes averaged $t_{1/2}$ values for the increasing (cellular K^+ release) and decreasing (K^+ reuptake) phases of the fluorescence profile. Though the $t_{1/2}$ for the fluorescence release phase was slightly greater in AQP4 null mice, the $t_{1/2}$ for the reuptake phase was remarkably greater (57 vs. 32 s, $P<0.001$), providing evidence for impaired glial cell K^+ uptake from the ECS in AQP4 deficiency. Further work is needed to define quantitatively the roles of altered ECS volume vs. K^+ uptake in the altered neural transduction phenotypes associated with AQP deficiency.

In related work, Puwarawuttipanit et al. studied hippocampal slices from α-syntrophin-deficient mice, in which membrane localization of AQP4 is partially reduced [61], and found a deficit in extracellular K^+ clearance following evoked neuronal activity. In addition, using a hyperthermia model of seizure induction, they found more of the α-syntrophin-deficient mice had more severe seizures than wild-type mice [62]. These data are consistent with the idea that AQP4 and its molecular partners (e.g. Kir4.1, α-syntrophin, dystrophin) together comprise a multifunctional 'unit' responsible for clearance of K^+ and/or H_2O following neural activity.

5. Summary and perspective

Phenotype analysis of AQP4-null mice has confirmed the involvement of AQP4 in cytotoxic brain edema, and provided strong evidence for unexpected roles of AQP4 in vasogenic brain edema, glial cell migration, and neural signal transduction. AQP4 facilitates clinically important water movement into and out of the brain in the development and resolution of brain edema; however, the precise mechanisms of water-salt coupling in removal of excess brain water across glia limitans remain unresolved. The phenotype data suggest AQP4 inhibition by small-molecules or other agents to reduce the accumulation of excess brain water in cytotoxic edema in stroke and some types of infections. AQP4 induction/activation is predicted to reduce brain water accumulation in vasogenic edema in brain tumor, focal abscess, and hydrocephalus, as well as accelerate the clearance of excess of brain water during the resolution phase of stroke and other forms of cytotoxic brain edema. Modulation of AQP4 expression or function is also predicted to modulate glial scar formation, which may be of clinical utility in traumatic injury, tumor and infection. For example, reduced glial scarring may facilitate axonal growth and access of chemotherapeutic agents to a lesion. AQP4 expression in high-grade glia-derived brain tumors may facilitate their local invasiveness, providing a rationale for AQP4 inhibition in therapy of some glioblastomas. AQP4 also appears also to be crucial for brain water and ion homeostasis during rapid neural activity; however, the precise mechanisms linking AQP4 expression to altered neural signaling remain unclear. Our recent data suggest increased extracellular space volume in AQP4 deficiency and impaired K^+ reuptake by AQP4-deficient astrocytes, which may be related to functionally significant AQP4-K^+ channel interactions. The seizure phenotype data in AQP4-null mice suggest the possibility of AQP4 modulation in epilepsy therapy, though the dual consequence of AQP4 modulation on seizure threshold and duration/severity may complicate such therapy. Thus, though there remain many basic mechanistic questions about the involvement of AQP4 in brain functions, there are exciting possibilities for AQP4-based therapy in a variety of common disorders of the central nervous system.

References

[1] R.A. Fishman, Brain edema, N. Engl. J. Med. 293 (1975) 706–711.
[2] L.H. Weed, P.S. McKibben, Experimental alteration of brain bulk, Am. J. Physiol. 48 (1919) 531–558.
[3] H. Hasegawa, T. Ma, W. Skach, M.A. Matthay, A.S. Verkman, Molecular cloning of a mercurial-insensitive water channel expressed in selected water-transporting tissues, J. Biol. Chem. 269 (1994) 5497–5500.
[4] B. Yang, T. Ma, A.S. Verkman, cDNA cloning, gene organization, and chromosomal localization of a human mercurial insensitive water channel. Evidence for distinct transcriptional units, J. Biol. Chem. 270 (1995) 22907–22913.
[5] S. Nielsen, E.A. Nagelhus, M. Amiry-Moghaddam, C. Bourque, P. Agre, O.P. Ottersen, Specialized membrane domains for water transport in glial cells: high-resolution immunogold cytochemistry of aquaporin-4 in rat brain, J. Neurosci. 17 (1997) 171–180.
[6] J.E. Rash, T. Yasumura, C.S. Hudson, P. Agre, S. Nielsen, Direct immunogold labeling of aquaporin-4 in square arrays of astrocyte and ependymocyte plasma membranes in rat brain and spinal cord, Proc. Natl. Acad. Sci. U. S. A. 95 (1998) 11981–11986.
[7] K. Oshio, D.K. Binder, B. Yang, S. Schecter, A.S. Verkman, G.T. Manley, Expression of aquaporin water channels in mouse spinal cord, Neuroscience 127 (2004) 685–693.
[8] L. Vitellaro-Zuccarello, S. Mazzetti, P. Bosisio, C. Monti, S. De Biasi, Distribution of Aquaporin 4 in rodent spinal cord: relationship with astrocyte markers and chondroitin sulfate proteoglycans, Glia 51 (2005) 148–159.
[9] A. Frigeri, M.A. Gropper, F. Umenishi, M. Kawashima, D. Brown, A.S. Verkman, Localization of MIWC and GLIP water channel homologs in neuromuscular, epithelial and glandular tissues, J. Cell Sci. 108 (1995) 2993–3002.
[10] B. Yang, D. Brown, A.S. Verkman, The mercurial insensitive water channel (AQP-4) forms orthogonal arrays in stably transfected Chinese hamster ovary cells, J. Biol. Chem. 271 (1996) 4577–4580.
[11] J.M. Verbavatz, T. Ma, R. Gobin, A.S. Verkman, Absence of orthogonal arrays in kidney, brain and muscle from transgenic knockout mice lacking water channel aquaporin-4, J. Cell Sci. 110 (1997) 2855–2860.
[12] T. Ma, B. Yang, A. Gillespie, E.J. Carlson, C.J. Epstein, A.S. Verkman, Generation and phenotype of a transgenic knockout mouse lacking the mercurial-insensitive water channel aquaporin-4, J. Clin. Invest. 100 (1997) 957–962.
[13] G.T. Manley, M. Fujimura, T. Ma, N. Noshita, F. Filiz, A.W. Bollen, P. Chan, A. S. Verkman, Aquaporin-4 deletion in mice reduces brain edema after acute water intoxication and ischemic stroke, Nat. Med. 6 (2000) 159–163.
[14] M.C. Papadopoulos, G.T. Manley, S. Krishna, A.S. Verkman, Aquaporin-4 facilitates reabsorption of excess fluid in vasogenic brain edema, FASEB J. 18 (2004) 1291–1293.
[15] I. Klatzo, Evolution of brain edema concepts, Acta Neurochir., Suppl. (Wien) 60 (1994) 3–6.
[16] H.K. Kimelberg, Current concepts of brain edema. Review of laboratory investigations, J. Neurosurg. 83 (1995) 1051–1059.
[17] A. Marmarou, G. Hochwald, T. Nakamura, K. Tanaka, J. Weaver, J. Dunbar, Brain edema resolution by CSF pathways and brain vasculature in cats, Am. J. Physiol. 267 (1994) H514–H520.
[18] H.J. Reulen, R. Graham, M. Spatz, I. Klatzo, Role of pressure gradients and bulk flow in dynamics of vasogenic brain edema, J. Neurosurg. 46 (1977) 24–35.

[19] E.I. Solenov, L. Vetrivel, K. Oshio, G.T. Manley, A.S. Verkman, Optical measurement of swelling and water transport in spinal cord slices from aquaporin null mice, J. Neurosci. Methods 113 (2002) 85–90.
[20] J.R. Thiagarajah, M.C. Papadopoulos, A.S. Verkman, Noninvasive early detection of brain edema in mice by near-infrared light scattering, J. Neurosci. Res. 80 (2005) 293–299.
[21] E. Solenov, H. Watanabe, G.T. Manley, A.S. Verkman, Sevenfold-reduced osmotic water permeability in primary astrocyte cultures from AQP-4-deficient mice, measured by a fluorescence quenching method, Am. J. Physiol., Cell Physiol. 286 (2004) C426–C432.
[22] M.C. Papadopoulos, A.S. Verkman, Aquaporin-4 gene disruption in mice reduces brain swelling and mortality in pneumococcal meningitis, J. Biol. Chem. 280 (2005) 13906–13912.
[23] Z. Vajda, M. Pedersen, E.M. Fuchtbauer, K. Wertz, H. Stodkilde-Jorgensen, E. Sulyok, T. Doczi, J.D. Neely, P. Agre, J. Frokiaer, S. Nielsen, Delayed onset of brain edema and mislocalization of aquaporin-4 in dystrophin-null transgenic mice, Proc. Natl. Acad. Sci. U. S. A. 99 (2002) 13131–13136.
[24] B. Nico, A. Frigeri, G.P. Nicchia, P. Corsi, D. Ribatti, F. Quondamatteo, R. Herken, F. Girolamo, A. Marzullo, M. Svelto, L. Roncali, Severe alterations of endothelial and glial cells in the blood-brain barrier of dystrophic mdx mice, Glia 42 (2003) 235–251.
[25] O. Bloch, M.C. Papadopoulos, G.T. Manley, A.S. Verkman, Aquaporin-4 gene deletion in mice increases focal edema associated with staphylococcal brain abscess, J. Neurochem. 95 (2005) 254–262.
[26] N.J. Abbott, Evidence for bulk flow of brain interstitial fluid: significance for physiology and pathology, Neurochem. Int. 45 (2004) 545–552.
[27] M.W. Brightman, The brain's interstitial clefts and their glial walls, J. Neurocytol. 31 (2002) 595–603.
[28] O. Bloch, G.T. Manley, A.S. Verkman.Accelerated progression of kaolin-induced hydrocephalus in aquaporin-4 deficient mice, J. Cereb. Blood Flow Metab. (in press)
[29] S. Saadoun, M.C. Papadopoulos, M. Hara-Chikuma, A.S. Verkman, Impairment of angiogenesis and cell migration by targeted aquaporin-1 gene disruption, Nature 434 (2005) 786–792.
[30] D.W. Hampton, K.E. Rhodes, C. Zhao, R.J. Franklin, J.W. Fawcett, The responses of oligodendrocyte precursor cells, astrocytes and microglia to a cortical stab injury, in the brain, Neuroscience 127 (2004) 813–820.
[31] C.F. Zhou, J.M. Lawrence, R.J. Morris, G. Raisman, Migration of host astrocytes into superior cervical sympathetic ganglia autografted into the septal nuclei or choroid fissure of adult rats, Neuroscience 17 (1986) 815–827.
[32] K.E. Rhodes, L.D. Moon, J.W. Fawcett, Inhibiting cell proliferation during formation of the glial scar: effects on axon regeneration in the CNS, Neuroscience 120 (2003) 41–56.
[33] K. Wang, L.K. Bekar, K. Furber, W. Walz, Vimentin-expressing proximal reactive astrocytes correlate with migration rather than proliferation following focal brain injury, Brain Res. 1024 (2004) 193–202.
[34] J.R. Faulkner, J.E. Herrmann, M.J. Woo, K.E. Tansey, N.B. Doan, M.V. Sofroniew, Reactive astrocytes protect tissue and preserve function after spinal cord injury, J. Neurosci. 24 (2004) 2143–2155.
[35] T.G. Bush, N. Puvanachandra, C.H. Horner, A. Polito, T. Ostenfeld, C.N. Svendsen, L. Mucke, M.H. Johnson, M.V. Sofroniew, Leukocyte infiltration, neuronal degeneration, and neurite outgrowth after ablation of scar-forming, reactive astrocytes in adult transgenic mice, Neuron 23 (1999) 297–308.
[36] J. Silver, J.H. Miller, Regeneration beyond the glial scar, Nat. Rev., Neurosci. 5 (2004) 146–156.
[37] T. Roitbak, E. Sykova, Diffusion barriers evoked in the rat cortex by reactive astrogliosis, Glia 28 (1999) 40–48.
[38] S. Saadoun, M.C. Papadopoulos, H. Watanabe, D. Yan, G.T. Manley, A.S. Verkman, Involvement of aquaporin-4 in astroglial cell migration and glial scar formation, J. Cell Sci. 118 (2005) 5691–5698.
[39] A. Schwab, Function and spatial distribution of ion channels and transporters in cell migration, Am. J. Physiol., Renal. Physiol. 280 (2001) F739–F747.
[40] G.F. Oster, A.S. Perelson, The physics of cell motility, J. Cell Sci., Suppl. 8 (1987) 35–54.
[41] J. Condeelis, A. Bresnick, M. Demma, S. Dharmawardhane, R. Eddy, A.L. Hall, R. Sauterer, V. Warren, Mechanisms of amoeboid chemotaxis: an evaluation of the cortical expansion model, Dev. Genet. 11 (1990) 333–340.
[42] M. Klein, P. Seeger, B. Schuricht, S.L. Alper, A. Schwab, Polarization of Na^+/H^+ and $Cl^-/HCO3^-$ exchangers in migrating renal epithelial cells, J. Gen. Physiol. 115 (2000) 599–608.
[43] A. Huttenlocher, Cell polarization mechanisms during directed cell migration, Nat. Cell Biol. 7 (2005) 336–337.
[44] C. Nicholson, Volume transmission in the year 2000, Prog. Brain Res. 125 (2000) 437–446.
[45] E. Sykova, Neuroscientist 3 (1997) 28–41.
[46] R. Piet, L. Vargova, E. Sykova, D.A. Poulain, S.H. Oliet, Physiological contribution of the astrocytic environment of neurons to intersynaptic crosstalk, Proc. Natl. Acad. Sci. U. S. A. 101 (2004) 2151–2155.
[47] J. Grosche, V. Matyash, T. Moller, A. Verkhratsky, A. Reichenbach, H. Kettenmann, Nat. Neurosci. 2 (1999) 139–143.
[48] E.A. Newman, Calcium signaling in retinal glial cells and its effect on neuronal activity, Prog. Brain Res. 132 (2001) 241–254.
[49] R.D. Fields, B. Stevens-Graham, New insights into neuron–glia communication, Science 298 (2002) 556–562.
[50] M. Nedergaard, B. Ransom, S.A. Goldman, New roles for astrocytes: redefining the functional architecture of the brain, Trends Neurosci. 26 (2003) 523–530.
[51] S.C. Lin, D.E. Bergles, Synaptic signaling between neurons and glia, Glia 47 (2004) 290–298.
[52] R. Jabs, T. Pivneva, K. Huttmann, A. Wyczynski, C. Nolte, H. Kettenmann, C. Steinhauser, Synaptic transmission onto hippocampal glial cells with hGFAP promoter activity, J. Cell Sci. 118 (2005) 3791–3803.
[53] J. Li, A.S. Verkman, Impaired hearing in mice lacking aquaporin-4 water channels, J. Biol. Chem. 276 (2001) 31233–31237.
[54] J. Li, R.V. Patil, A.S. Verkman, Mildly abnormal retinal function in transgenic mice without Muller cell aquaporin-4 water channels, Investig. Ophthalmol. Vis. Sci. 43 (2002) 573–579.
[55] D.K. Binder, K. Oshio, T. Ma, A.S. Verkman, G.T. Manley, Increased seizure threshold in mice lacking aquaporin-4 water channels, NeuroReport 15 (2004) 259–262.
[56] D.K. Binder, X. Yao, T.J. Sick, A.S. Verkman, G.T. Manley, Increased seizure duration and slowed potassium kinetics in mice lacking aquaporin-4 water channels, Glia 53 (2006) 631–636.
[57] D.K. Binder, M.C. Papadopoulos, P.M. Haggie, A.S. Verkman, In vivo measurement of brain extracellular space diffusion by cortical surface photobleaching, J. Neurosci. 24 (2004) 8049–8056.
[58] M.C. Papadopoulos, D.K. Binder, A.S. Verkman, Enhanced macromolecular diffusion in brain extracellular space in mouse models of vasogenic edema measured by cortical surface photobleaching, FASEB J. 19 (2005) 425–427.
[59] M.C. Papadopoulos, J.K. Kim, A.S. Verkman, Extracellular space diffusion in central nervous system: anisotropic diffusion measured by elliptical surface photobleaching, Biophys. J. 89 (2005) 3660–3668.
[60] P. Padmawar, X. Yao, O. Bloch, G.T. Manley, A.S. Verkman, K^+ waves in brain cortex visualized using a long-wavelength K^+-sensing fluorescent indicator, Nat. Methods 2 (2005) 825–827.
[61] W. Puwarawuttipanit, A.D. Bragg, D.S. Frydenlund, M.N. Mylonakou, E. A. Nagelhus, M.F. Peters, N. Kotchabhakdi, M.E. Adams, S.C. Froehner, F.M. Haug, O.P. Ottersen, M. Amiry-Moghaddam, Differential effect of alpha-syntrophin knockout on aquaporin-4 and Kir4.1 expression in retinal macroglial cells in mice, Neuroscience 139 (2006) 165–175.
[62] M. Amiry-Moghaddam, A. Williamson, M. Palomba, T. Eid, N.C. de Lanerolle, E.A. Nagelhus, M.E. Adams, S.C. Froehner, P. Agre, O.P. Ottersen, Delayed K^+ clearance associated with aquaporin-4 mislocalization: phenotypic defects in brains of alpha-syntrophin-null mice, Proc. Natl. Acad. Sci. U. S. A. 100 (2003) 13615–13620.